

## Research Article

# Modelling and Deliberation of Multireinforcement Surface on Tribothermal Adsorption Performance of Nickel Alloy Matrix Hybrid Nanocomposite

G. Ramya Devi,<sup>1</sup> C. B. Priya ,<sup>2</sup> C. Dineshbabu,<sup>3</sup> R. Karthick,<sup>4</sup> K. Thanigavelmurugan,<sup>5</sup> and Prabhu Paramasivam <sup>6</sup>

<sup>1</sup>Department of Mechanical Engineering, Saveetha School of Engineering, SIMATS, Chennai, 602105 Tamil Nadu, India

<sup>2</sup>Department of Production, National Institute of Technology, 620015, Trichy, Tamil Nadu, India

<sup>3</sup>Department of Mechanical Engineering, Kongunadu College of Engineering and Technology, Trichy, 621215 Tamil Nadu, India

<sup>4</sup>Department of Mechanical Engineering, M. Kumarasamy College of Engineering, Karur, 639113 Tamil Nadu, India

<sup>5</sup>Department of Mechanical Engineering, Loyola Institute of Technology, Chennai, 600123 Tamil Nadu, India

<sup>6</sup>Department of Mechanical Engineering, College of Engineering and Technology, Mattu University, 318, Ethiopia

Correspondence should be addressed to Prabhu Paramasivam; [prabhuparamasivam21@gmail.com](mailto:prabhuparamasivam21@gmail.com)

Received 25 August 2022; Revised 9 October 2022; Accepted 14 October 2022; Published 26 November 2022

Academic Editor: Debabrata Barik

Copyright © 2022 G. Ramya Devi et al. This is an open access article distributed under the Creative Commons Attribution License, which permits unrestricted use, distribution, and reproduction in any medium, provided the original work is properly cited.

The present research work is aimed at developing a nickel alloy (Ni-Cr) matrix hybrid nanocomposite comprising 5 wt%, 10 wt%, and 15 wt% of alumina nanoparticles ( $\text{Al}_2\text{O}_3$ ) size of 50 nm with stable weight percentage (5 wt%) of titanium dioxide ( $\text{TiO}_2$ ) nanoparticle via vacuum die casting process for an automobile brake pad application. The deliberation of multireinforcement surface on nickel alloy matrix tribological performance was evaluated by constant sliding distance (200 m) on dry sliding condition via rotating pin on disc apparatus with different loading conditions of 10 N, 30 N, 50 N, and 70 N under the sliding velocity of 0.25 m/sec, 0.5 m/sec, and 0.75 m/sec, respectively. The influences of alumina and titanium dioxide nanoparticles in the nickel alloy matrix resulted in the thermal conductivity increasing by 18% compared to unreinforced nickel alloy. After temperature drop, the coefficient of thermal expansion for nickel alloy hybrid composite decreases progressively with increased reinforcement content as 10 wt%  $\text{Al}_2\text{O}_3$ /5 wt%  $\text{TiO}_2$ . Further inclusion of both  $\text{Al}_2\text{O}_3$  and  $\text{TiO}_2$  in nickel alloy was increased nominally. The thermal adsorption characteristic on composites mass loss was decreased while temperature increased from 28°C to 1000°C.

## 1. Introduction

The innovative creation of conventional matrix materials (aluminium, magnesium, and titanium) was blended with organic/inorganic reinforcements to achieve specific characteristics such as high wear resistance [1]; good thermal stability on higher temperatures [2]; high tensile strength; and good corrosion resistance facilitates in a sports car, aviation, electrical contacts, and structural applications [3]. The incorporation of hard ceramic particles into metal matrix speaks with tremendous isotropic performance compared to conventional materials [4, 5]. Similarly, selecting matrix,

reinforcement, and process parameters for composite fabrication was the most critical factor for deciding composite characteristics [6, 7]. Recently, most researchers referred to aluminium, magnesium, titanium, and their alloy matrix developed with organic/inorganic reinforcement [8] via conventional fabrication techniques such as solid and liquid state processing [9, 10]. Nickel and its alloy-based matrix materials have met the demand for high-temperature applications like automobile valves, brake pads, and siphon bodies [11]. In the past decades, various researches have been accomplished by tribomechanical performance studies on nickel-based alloy matrices such as nickel (Ni)/chromium

TABLE 1: Thermomechanical characteristics of matrix and reinforcements.

| Descriptions   | Materials/properties           | Density<br>g/cc | Hardness<br>VHN | Modulus of elasticity<br>GPa | Melting point<br>°C | Thermal conductivity<br>W/mK |
|----------------|--------------------------------|-----------------|-----------------|------------------------------|---------------------|------------------------------|
| Matrix         | Ni-Cr alloy                    | 7.75            | 204             | 110                          | 1475                | 17                           |
| Reinforcements | Al <sub>2</sub> O <sub>3</sub> | 3.96            | 1365            | 370                          | 2054                | 30                           |
|                | TiO <sub>2</sub>               | 4.23            | 713             | 37.5                         | 1843                | 0.62                         |

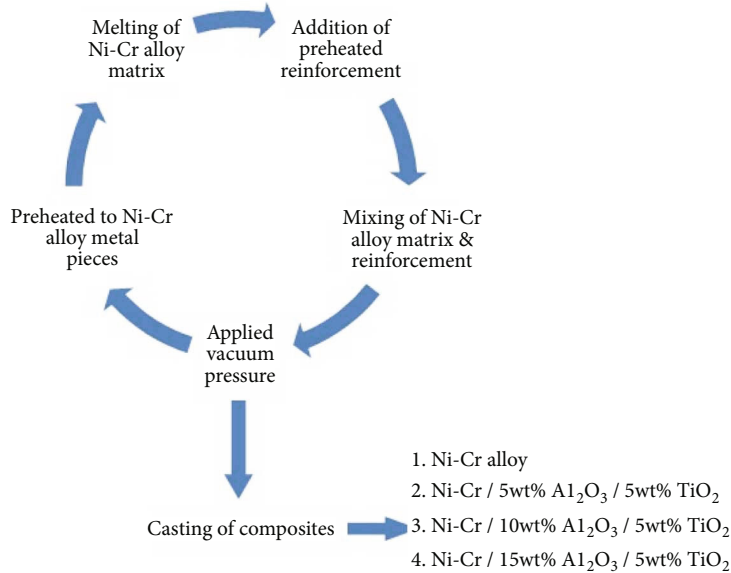


FIGURE 1: Schematic diagram for processing of Ni-Cr alloy matrix hybrid nanocomposite.

TABLE 2: Constitutions of Ni-Cr alloy matrix hybrid nanocomposite.

| Sample | Ni-Cr | Weight percentage in %         |                  | TiC |
|--------|-------|--------------------------------|------------------|-----|
|        |       | Al <sub>2</sub> O <sub>3</sub> | TiO <sub>2</sub> |     |
| 1      | 100   | 0                              | 0                | 0   |
| 2      | 90    | 5                              | 5                | 5   |
| 3      | 85    | 10                             | 5                | 5   |
| 4      | 80    | 15                             | 5                | 5   |

(Cr)/zirconia matrix [12], Ni/Cr/MoS<sub>2</sub>, nickel (Ni)/graphite (Gr)/titanium carbide (TiC), Ni/tungsten carbide (WC), Ni/titanium carbide (TiC), and Ni/cobalt (Co)/zirconia [13]. However, the properties of composite were integrated by ceramic phase (Si<sub>3</sub>N<sub>4</sub>, Al<sub>2</sub>O<sub>3</sub>, SiC, ZrO<sub>2</sub>, etc.) [14], high-performance materials (Co, Fe, Ni, etc.) [15–17], and intermetallic compounds alloys (Ti-Al, Fe-Al, Ni-Al, etc.) [18–20]. The tribological behaviour of Ni/Cr alloy was investigated at higher temperatures (20–600°C). It resulted in oxide sulfides during wear surface under reduced friction [21]. The Ni/TiC composite was developed through the Gr coating process. The Gr-coated layer in Ni/TiC composite has low wear loss and better coefficient friction than conventional Ni-Cr alloy [22]. Leech et al. [23] investigated the wear performance of Ni/TiC alloy composite by dry state pin on flat wear tester with a garnet abrasive wheel. They

found that the composite has superior wear performance on higher frictional temperature excavation on the constituent matrix. Incorporating TiC particles leads to resisting the depletion against the frictional temperature. The TiC-reinforced Ni-Cr alloy composite was produced by infiltration technique, and its electrical-thermal-wear characteristics were studied for high-temperature applications. TiC particles in the Ni matrix having good tribothermal behaviour resist the high frictional force during the evaluation of wear studies [24]. Srivastava et al. [25] studied the mechanical and chemical properties of zirconia bonded Ni-Co alloy composite. They found that the composite has good chemical and mechanical performance. Among the studies reported above, limited research is available on tribothermal adsorption on multiceramic reinforced nickel alloy hybrid nanocomposite. The present research is focused on developing a nickel alloy matrix bonded with various weight percentages of Al<sub>2</sub>O<sub>3</sub> and stable weight percentages of TiO<sub>2</sub> via a vacuum die casting process. Finally, the developed composites' tribothermal performance was evaluated by ASTM test standards. The test results were compared to cast nickel alloy and recommended for brake pad applications.

## 2. Materials and Processing of Composites

*2.1. Materials and Reinforcement.* Ni-Cr alloy metals are pointed out for their superior tribomechanical characteristics

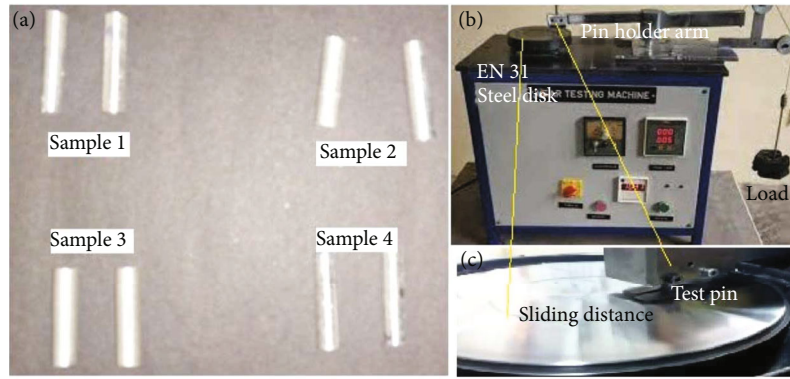


FIGURE 2: Dry state wear test apparatus setup: (a) test pin samples, (b) wear tester, and (c) enlarged view of test pin and rotating disk.

TABLE 3: Wear test input process parameters.

| Parameters | Sliding distance | Sliding speed             | Load                 |
|------------|------------------|---------------------------|----------------------|
| Unit       | 200 m            | 0.25, 0.5, and 0.75 m/sec | 10, 30, 50, and 70 N |

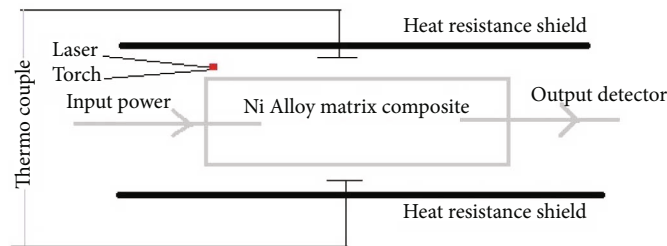


FIGURE 3: Block diagram for laser-based thermal conductivity evaluation.

TABLE 4: Wear performance Ni-Cr alloy matrix hybrid nanocomposite.

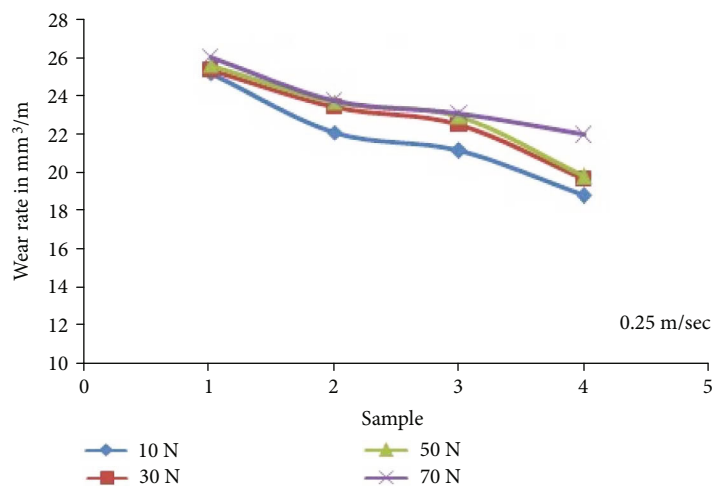
| Sample | Wear performance on 0.25 m/sec at 70 N load   |      |                       |                   |
|--------|-----------------------------------------------|------|-----------------------|-------------------|
|        | Wear rate $\times 10^{-3}$ mm <sup>3</sup> /m | COF  | Frictional force in N | Temperature in °C |
| 1      | 26.12                                         | 0.29 | 58.12                 | 57                |
| 2      | 23.81                                         | 0.37 | 62.17                 | 59                |
| 3      | 23.12                                         | 0.39 | 67.43                 | 64                |
| 4      | 21.98                                         | 0.41 | 69.43                 | 68                |

and excellent corrosion resistance. So the nickel alloy was chosen as matrix material with 20% chromium [26]. The different weight percentages of 50 nm alumina ( $\text{Al}_2\text{O}_3$ ) and stable weight percentage of  $\text{TiO}_2$  nanoparticles were considered to reinforce the Ni-Cr alloy matrix. The  $\text{Al}_2\text{O}_3$  has good wear resistance, the best electrical insulator, and high thermal stability.  $\text{TiO}_2$  particles were one of the best complex reinforcements bonded to the Ni-Cr alloy matrix, resulting in good chemical stability and high thermal stability [27]. Table 1 indicates the thermomechanical properties of matrix and reinforcements.

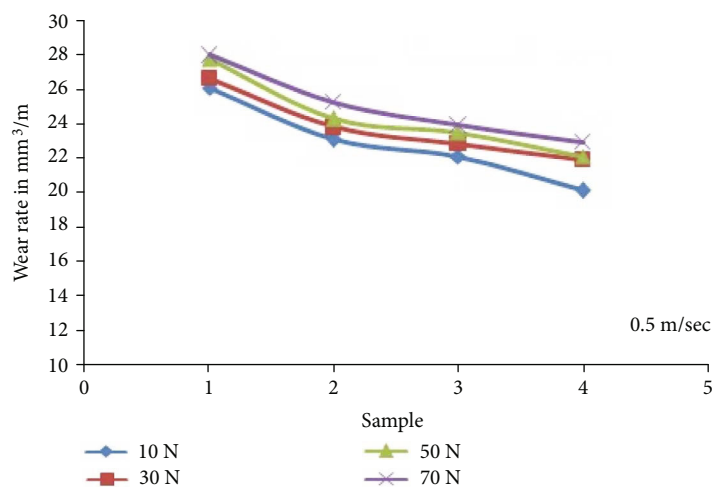
## 2.2. Experimental Details for Processing and Testing of Ni-Cr Alloy Matrix Composites.

The processing of Ni-Cr alloy matrix composite is represented in Figure 1. The different sized Ni-Cr alloy pieces are located in an electrical furnace configured with an induction coil with the capacity of 5 kg operated under a different temperature range of 27°C to 1700°C. The preheated temperature of Ni-Cr alloy is maintained at 400°C in stable condition on 15 min period [28]. Then, the furnace temperature is raised from 1200°C to 1500°C to melt the Ni-Cr alloy as molten (liquids) stage. Similarly, the reinforcements are preheated at 550°C to remove the moisture content and increase the wettability [29]. The externally preheated reinforcements are added into the semisolid stage (1100°C) Ni-Cr alloy, and both matrix and reinforcements are bonded with the help of stir action (400 rpm) for a 10 min period. The prepared Ni-Cr alloy matrix was poured into preheated (450°C) rectangular die sized on 100 × 50 × 20 mm with an applied vacuum pressure of  $2 \times 10^5$  Pa [29]. The developed Ni-Cr alloy matrix composites are cooled by natural ambient temperature without an external medium. Finally, the composites are sized by 30 × 10 × 10 cm for tribological analysis. The constitutions of Ni-Cr alloy/reinforcements are mentioned in Table 2.

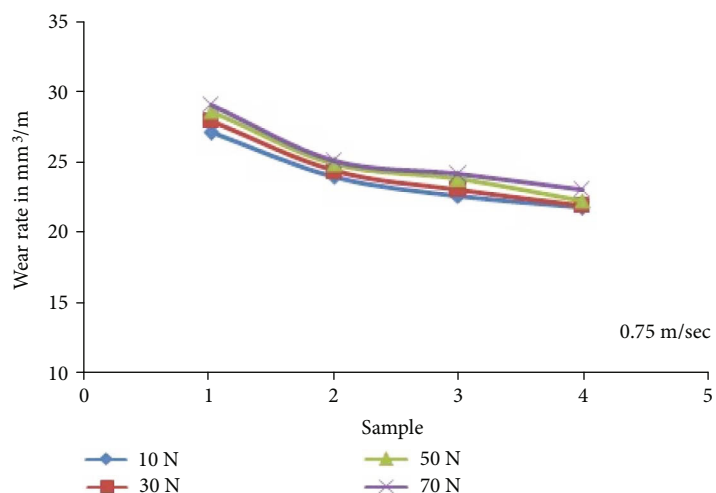
The dry state wear performance of unreinforced and reinforced Ni-Cr alloy composites (Figure 2(a)) was evaluated by ASTM G99-05 via pin-on-disk wear apparatus configured with EN31 steel counter disc is shown in Figure 2(b).



(a)

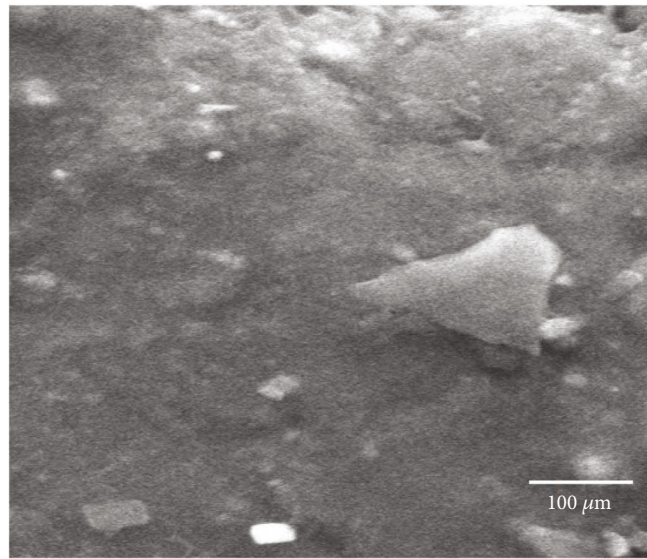


(b)



(c)

FIGURE 4: Continued.



(d)

FIGURE 4: Wear rate of Ni-Cr alloy matrix composites (a) 0.25 m/sec, (b) 0.5 m/sec, and (c) 0.75 m/sec. (d) Optical micrograph of Ni-Cr/15 wt%  $\text{Al}_2\text{O}_3$ /5 wt%  $\text{TiO}_2$  hybrid nanocomposite.

The wear test samples were sized by  $30 \text{ mm} \times 10 \text{ mm} \times 10 \text{ mm}$  and held vertically into the pin holder arm, as shown in Figure 2(c). All the test samples were tested by test room conditions like  $27^\circ\text{C}$  temperature with 50-62% relative humidity maintained by a constant sliding distance of 200 m under different load and sliding speed conditions mentioned in Table 3.

Figure 3 illustrates the principle diagram for evaluating thermal conductivity on Ni-Cr alloy matrix composite ( $10 \text{ mm} \times 50 \text{ mm}$ ) by laser beam source. The Jupiter STA 449/F3 model thermal analyzer was used to study the thermal behaviour of Ni-Cr alloy composites bonded with different reinforcements [29]. It was evaluated in an argon environment with a temperature range of  $150^\circ\text{C}$  to  $2400^\circ\text{C}$ . The laser flash method is to be adopted for finding the thermal conductivity ( $\kappa_{\text{Ni}}$ ) of the Ni matrix body referred as

$$\kappa_{\text{Ni}}(T) = \rho(T) \times \alpha(T) \times C_p(T), \quad (1)$$

where  $\kappa$  is the thermal conductivity,  $T$  is the temperature,  $\rho$  is the density of material,  $\alpha$  is the thermal diffusivity, and  $C_p$  is the specific heat coefficient.

The linear thermal expansion of the Ni-Cr alloy matrix hybrid nanocomposite was estimated using NETZSCH make DIL 402C and LFA 427 model thermotester apparatus.

### 3. Results and Discussion

**3.1. Effect  $\text{Al}_2\text{O}_3$  and  $\text{TiO}_2$  on Dry State Wear Performance of Ni-Cr Alloy Matrix Composite.** Table 4 shows the wear test results on Ni-Cr alloy matrix hybrid nanocomposite tested by dry state condition with 0.25 m/sec, 0.5 m/sec, and 0.75 m/sec sliding speed under an applied load of 10 N, 30 N, 50 N, and 70 N, respectively.

It was observed from Figures 4(a)–4(c) that the wear rate of Ni-Cr alloy composite decreased gradually with the additions of  $\text{Al}_2\text{O}_3$  and 5 wt%  $\text{TiO}_2$ . Figures 4(a)–4(c) illustrate the wear performance of Ni-Cr alloy containing 5 wt%, 10 wt%, and 15 wt% of  $\text{Al}_2\text{O}_3$  with constant 5 wt% of  $\text{TiO}_2$  hybrid nanocomposite evaluated by at 0.25 m/sec with different loading conditions like 10 N, 30 N, 50 N, and 70 N, respectively [30].

The composite having 15 wt% alumina nanoparticles with 5 wt% titanium dioxide particle shows an optimum wear resistance of  $21.98 \text{ mm}^3/\text{m}$  under high load 70 N. It was due to hard alumina's resistance to the deflection layer on the high frictional force. A similar trend was found during the wear evaluation of AZ61 magnesium alloy hybrid composites [7]. Figure 4(b) represents the wear rate of unreinforced and reinforced Ni-Cr alloy hybrid nanocomposite under 0.5 m/sec sliding velocity with varied load conditions of 10-70 N. It was clearly shown that the wear rate progressively increased with an increase in load condition at a constant sliding distance of 200 m [31]. Similar results were reported by León-Patiño et al. [24] during the evaluation of Ni/TiC composites. Figure 4(c) shows the variations of wear rate for Ni-Cr alloy hybrid nanocomposite estimated by a high sliding speed of 0.75 m/sec. It shows the wear rate of composite is  $29.12 \text{ mm}^3/\text{m}$  to  $22.98 \text{ mm}^3/\text{m}$  under 70 N applied load. However, the wear rate of the composite decreased with increased reinforcements. Good bonding strength between matrix and reinforcement is evidenced in Figure 4(d). However, interfacial bonding strength may be varied due to the choice of process (stir casting) parameter [5].

Figure 5 shows the coefficient of friction (COF) of Ni-Cr alloy and its hybrid nanocomposite estimated by 0.25 m/sec to 0.75 m/sec sliding velocity with varied load conditions of 10-70 N, respectively. Figure 5(a) illustrates that the

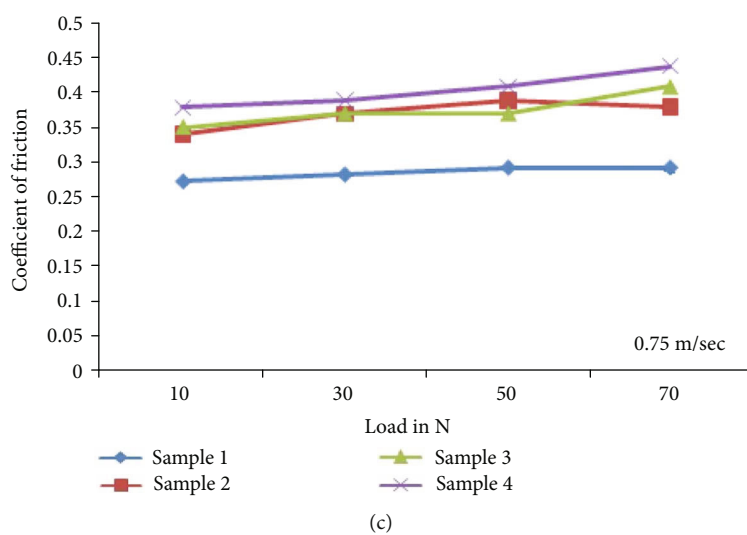
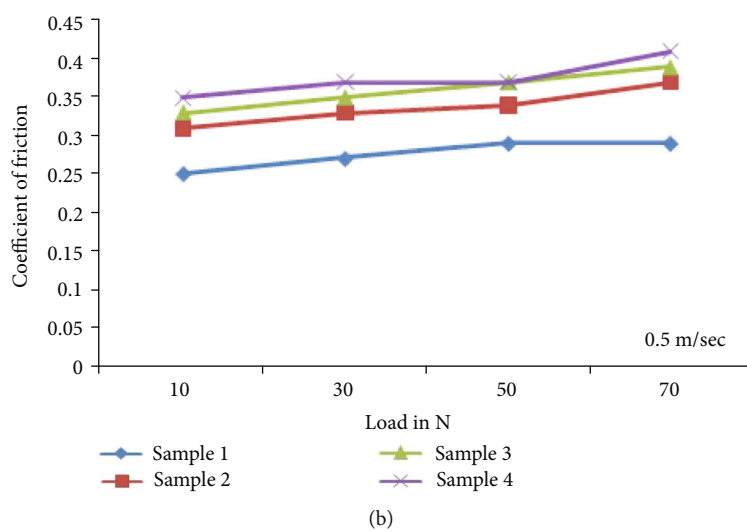
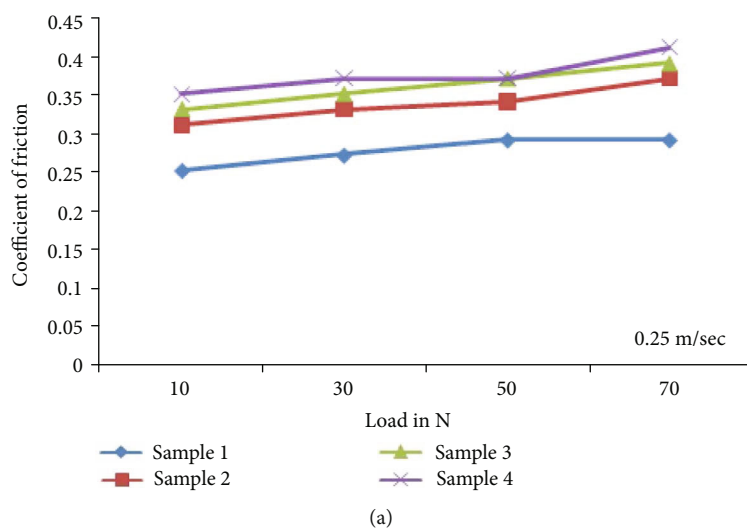


FIGURE 5: Continued.

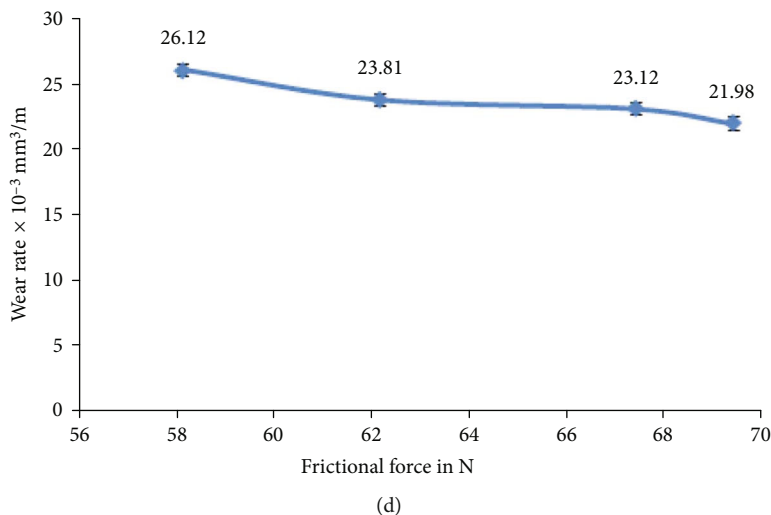


FIGURE 5: Coefficient of friction for Ni-Cr alloy matrix composites: (a) 0.25 m/sec, (b) 0.5 m/sec, and (c) 0.75 m/sec. (d) Effect of the frictional force on wear relation of Ni-Cr alloy hybrid nanocomposites.

coefficient of friction of unreinforced and reinforced Ni-Cr alloy composite varies from 0.25 to 0.41. The COF of composite has steadily increased with the additions of alumina nanoparticles and titanium dioxide particles. Figure 5(b) shows the COF of Ni-Cr alloy and its hybrid nanocomposite estimated by 0.5 m/sec sliding speed at different load conditions. The curve indicates that an upward slope varied from 0.34, 0.37, 0.39, and 0.41 on an applied load of 10 N, 30 N, 50 N, and 70 N, respectively. The improvement of COF was due to the presence of hard ceramic which leads to enhance the resistance of high frictional on the higher temperature of 57°C. The high sliding performance on COF of Ni-Cr alloy and its hybrid nanocomposite is shown in Figure 5(c). It was revealed from Figure 5(c) that the challenging ceramic plays a significant role in friction with a higher coefficient value of 0.44 under high load and sliding speed of 40 N and 0.75 m/sec with 73.6 N frictional force. However, the COF of the composite was increased progressively by adding reinforcement. The maximum COF is 0.44, found in sample 4. Its COF value increased 34% as compared to cast Ni-Cr alloy.

**3.2. Effect of the Frictional Force on Wear Performance of Ni-Cr Alloy Matrix Composites.** Figure 5(d) represents the relation of frictional force effect on wear behaviour of Ni-Cr alloy hybrid nanocomposite evaluated by 70 N load with the applied sliding speed of 0.25 m/sec.

It was revealed from Figure 5(d) that the composite's wear rate gradually decreased with an increased friction force of 58.12 N to 69.43 N. Sample 1 indicates that the wear rate of  $26.12 \times 10^{-3} \text{ mm}^3/\text{m}$  on an applied load of 70 N showed that 58.12 N frictional force liberates the 57°C, while compared to reinforced hybrid nanocomposite, the wear rate of Ni-Cr alloy has high. The Ni-Cr/15 wt%  $\text{Al}_2\text{O}_3$ /5 wt%  $\text{TiO}_2$  hybrid nanocomposite showed a minimum wear rate on high load under 0.25 m/sec sliding speed. The maximum frictional force of 69.43 N liberates the 68°C temperature and leads to abrasive wear, so the rigid reinforcements resist the

particle dislocation during high sliding force. So the wear rate of the composite was reduced, and the coefficient of friction was increased. Similarly, the past literature studies on the wear behaviour of Ni-Cr alloy showed an increased friction coefficient at high frictional temperatures.

**3.3. Effect  $\text{Al}_2\text{O}_3$  and  $\text{TiO}_2$  on Thermal Adsorption Behaviour of Ni-Cr Alloy Matrix Composite.** Table 5 represents the thermal adsorption behaviour of Ni-Cr alloy composite bonded with various weight percentages (5 wt%, 10 wt%, and 15 wt %) of  $\text{Al}_2\text{O}_3$  and 5 wt% of  $\text{TiO}_2$ .

Figure 6 indicates that the thermal conductivity of Ni-Cr alloy contained 5, 10, and 15 wt% of alumina nanoparticle with stable 5 wt% of  $\text{TiO}_2$ . Both nanoparticles have enhanced the thermal performance of the composite.

The thermal conductivity of composite has varied from 33.918  $\text{W}/\text{m}^\circ\text{C}$  to 41.870  $\text{W}/\text{m}^\circ\text{C}$  due to the inclusion of hard ceramic. The cast Ni-Cr bonding has 33.918  $\text{W}/\text{m}^\circ\text{C}$  while adding 5 wt% of hybrid constitutions was 37.829  $\text{W}/\text{m}^\circ\text{C}$ . Generally, alumina and titanium dioxide have good thermal stability and high hardness compared to conventional reinforcements [4]. The maximum thermal conductivity of 41.870  $\text{W}/\text{m}^\circ\text{C}$  was found on a composite containing 15 wt%  $\text{Al}_2\text{O}_3$ /5 wt%  $\text{TiO}_2$ . It was due to the effect weight percentages and good isotropic properties of Ni-Cr alloy. However, the thermal conductivity of Ni-Cr alloy and its composites may vary due to input temperature conditioning. The influences of alumina and titanium dioxide nanoparticles in the nickel alloy matrix resulted in the thermal conductivity increasing by 18% compared to unreinforced nickel alloy.

The thermal dimension of temperature variations of Ni-Cr alloy and its hybrid nanocomposite coefficient of thermal expansion (CTE) is represented in Figure 7. It was closely observed by the thermal changes of Ni-Cr alloy hybrid nanocomposite which may be related to the bonding of matrix and reinforcement. The CTE of Ni-Cr alloy was  $17 \times 10^{-6}$  and adding 5 and 10 wt%  $\text{Al}_2\text{O}_3$ /5 wt%  $\text{TiO}_2$  was 15

TABLE 5: Thermal behaviour of Ni-Cr alloy composite.

| Sample/units | Thermal adsorption performance Ni-Cr alloy matrix hybrid nanocomposites |                               |                                                       |                           |
|--------------|-------------------------------------------------------------------------|-------------------------------|-------------------------------------------------------|---------------------------|
|              | Constitutions                                                           | Thermal conductivity<br>W/m°C | Coefficient of thermal expansion<br>X10 <sup>-6</sup> | Wear loss on 1000°C<br>mg |
| 1            | Ni-Cr alloy                                                             | 33.918                        | 17                                                    | 9.78                      |
| 2            | Ni/5 wt% Al <sub>2</sub> O <sub>3</sub> /5 wt% TiO <sub>2</sub>         | 37.829                        | 15                                                    | 34.78                     |
| 3            | Ni/10 wt% Al <sub>2</sub> O <sub>3</sub> /5 wt% TiO <sub>2</sub>        | 39.619                        | 13                                                    | 54.32                     |
| 4            | Ni/15 wt% Al <sub>2</sub> O <sub>3</sub> /5 wt% TiO <sub>2</sub>        | 41.870                        | 15                                                    | 40.71                     |

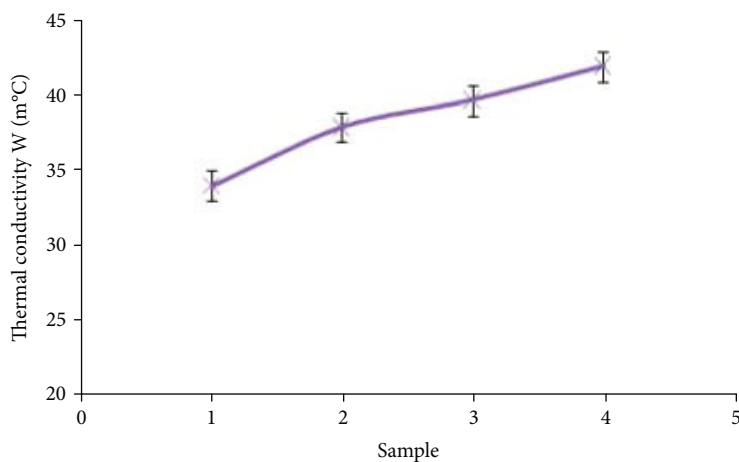


FIGURE 6: Thermal conductivity of Ni-Cr alloy matrix composites.

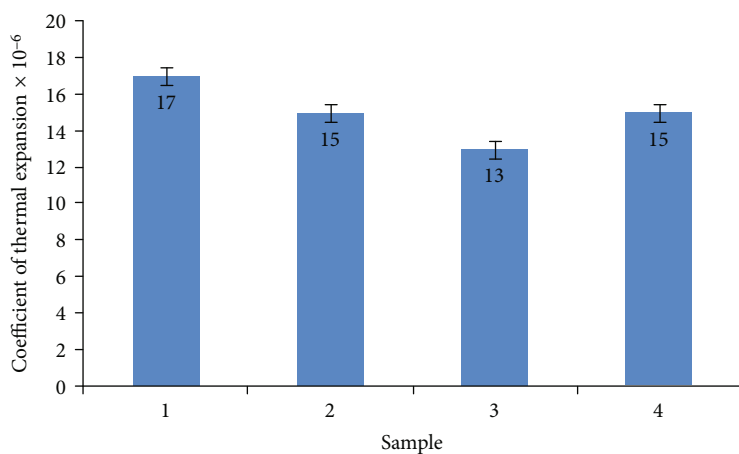


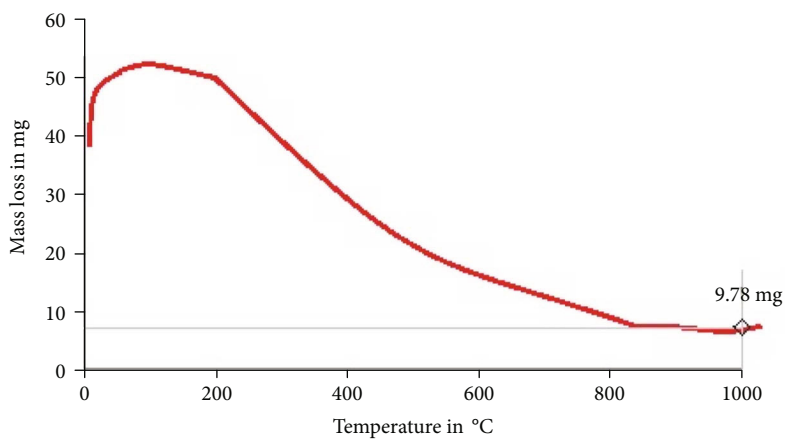
FIGURE 7: Coefficient of thermal expansion of Ni-Cr alloy matrix composites.

× 10<sup>-6</sup> and 13 × 10<sup>-6</sup>, respectively. It was due to the increased temperature of 30°C to 900°C. After that, the composite contained 15 wt% Al<sub>2</sub>O<sub>3</sub>/5 wt% TiO<sub>2</sub> hybrid nanocomposite with a thermal growth of (15 × 10<sup>-6</sup>). It happened due to its temperature drop from 900°C to 600°C. At this point, the thermal expansion was increased nominally. So, from the heating to cooling phase, the coefficient of thermal expansion for nickel alloy hybrid composite decreases progressively with increased reinforcement con-

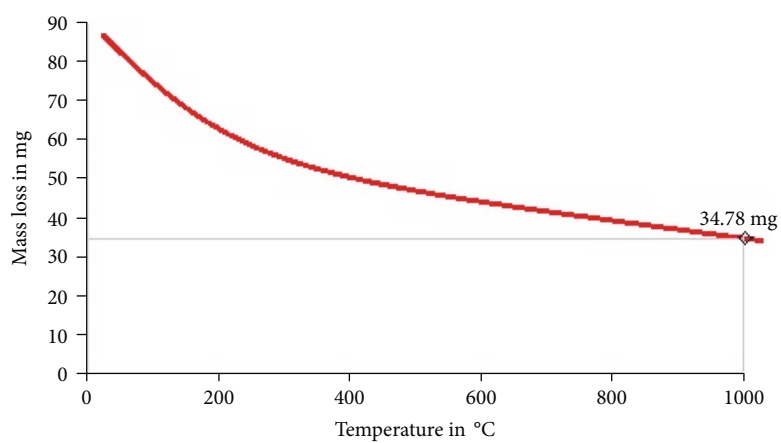
tent as 10 wt% Al<sub>2</sub>O<sub>3</sub>/5 wt% TiO<sub>2</sub>. Further inclusion of both Al<sub>2</sub>O<sub>3</sub> and TiO<sub>2</sub> in nickel alloy was increased nominally.

**3.4. Thermal Adsorption Characteristics.** The thermal adsorption characteristics of mass loss of Ni-Cr alloy and its hybrid nanocomposites were evaluated by thermogravimetric apparatus configured with 0°C to 1500°C temperature span under a constant heat flow rate of 25°C/min as shown in Figures 8(a)–8(d). The wear loss of Ni-Cr alloy was found

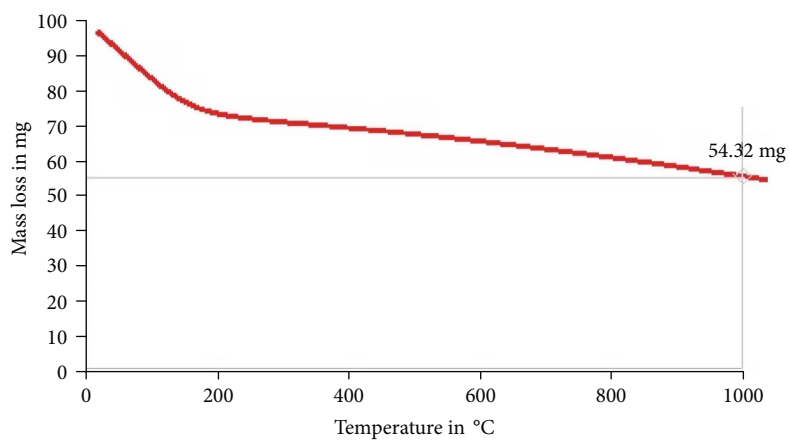




(a)



(b)



(c)

FIGURE 8: Continued.

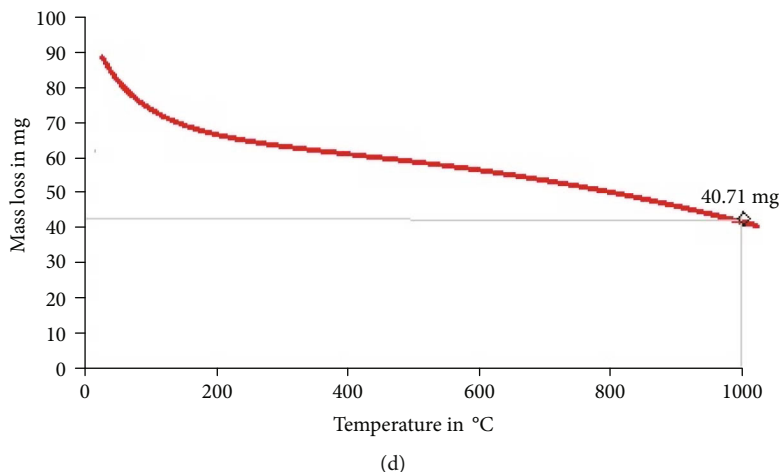


FIGURE 8: Thermal adsorption performance on wear loss of Ni-Cr alloy matrix composites: (a) cast Ni-Cr alloy, (b) Ni-Cr/5 wt%  $\text{Al}_2\text{O}_3$ /5 wt%  $\text{TiO}_2$ , (c) Ni-Cr/10 wt%  $\text{Al}_2\text{O}_3$ /5 wt%  $\text{TiO}_2$ , and (d) Ni-Cr/15 wt%  $\text{Al}_2\text{O}_3$ /5 wt%  $\text{TiO}_2$ .

at 9.78 mg on 1000°C under 25°C/min steady heat supply. At the same time, incorporating  $\text{Al}_2\text{O}_3$  and 5 wt% of  $\text{TiO}_2$  in the Ni-Cr matrix showed higher mass loss than Ni-Cr alloy. It was due to the effect of ceramic particles on different phases, like dislocation between the Ni-Cr layers. Figures 8(c) and 8(d) illustrate the effect of thermal adsorption on mass loss of hybrid nanocomposites containing 10 wt% and 15 wt% of alumina nanoparticles with stable 5 wt% of  $\text{TiO}_2$  particle, resulting in a limited mass loss on a higher temperature. The curve of Figure 8(d) indicates the regular slope of 926°C. Further temperature increases showed a steady-state condition of mass loss. It happened due to the chain reaction of hard ceramic particles that can withstand the high temperature on 25°C/min heat flow.

The weight loss of the hybrid nanocomposite (Ni-Cr/15 wt%  $\text{Al}_2\text{O}_3$ /5 wt%  $\text{TiO}_2$ ) was limited to 1.21 times of ambient temperature under the same heat flow of 25°C/min. However, the thermal adsorption on mass loss of composite is related to interfacial bonding strength between matrix and reinforcements of the hybrid nanocomposite.

#### 4. Conclusions

The vacuum die casting process developed the nickel alloy (Ni-Cr) matrix hybrid nanocomposites. The developed composites were subjected to tribothermal characteristics studies. Based on this performance, the composite containing 15 wt% alumina nanoparticles with 5 wt% titanium nanoparticles was found to have optimum tribological-thermal properties compared to conventional cast Ni-Cr alloy. The wear resistance of sample 4 is increased by 16% compared to cast Ni-Cr alloy. The coefficient of friction of 0.44 is observed on Ni-Cr alloy/15 wt% alumina nanoparticle with 5 wt% titanium nanoparticle under high sliding speed and a load of 0.75 m/sec and 70 N. The thermal conductivity of Ni-Cr alloy/15 wt%  $\text{Al}_2\text{O}_3$ /5 wt%  $\text{TiO}_2$  hybrid nanocomposite found 18% increased conductivity compared to Ni-Cr alloy. However, the composite containing 15 wt%  $\text{Al}_2\text{O}_3$ /5 wt%  $\text{TiO}_2$  shows  $15 \times 10^{-6}$ , and its CTE decreased to 11% compared

to Ni-Cr alloy. It was due to the reason that decreased CTE was related to bonding strength between Ni-Cr alloy and ceramist. The thermal adsorption performance on weight loss of hybrid nanocomposite (Ni-Cr/15 wt%  $\text{Al}_2\text{O}_3$ /5 wt%  $\text{TiO}_2$ ) was limited to 1.21 times ambient temperature under the heat flow rate of 25°C/min.

#### Data Availability

The data used to support the findings of this study are included within the article. Should further data or information be required, these are available from the corresponding author upon request.

#### Conflicts of Interest

The authors declare that there are no conflicts of interest regarding the publication of this paper.

#### References

- [1] S. J. Komarneni, "Nanocomposites," *Journal of Materials Chemistry C, Materials for Optical and Electronic Devices*, vol. 2, no. 12, pp. 1219–1219, 1992.
- [2] L. Natrayan and M. Senthil Kumar, "Influence of silicon carbide on tribological behaviour of AA2024/ $\text{Al}_2\text{O}_3$ /SiC/Gr hybrid metal matrix squeeze cast composite using Taguchi technique," *Materials Research Express*, vol. 6, no. 12, article 1265f9, 2019.
- [3] D. S. Prasad and C. Shoba, "Hybrid composites - a better choice for high wear resistant materials," *Journal of Material Research Technology*, vol. 3, no. 2, pp. 172–178, 2014.
- [4] F. Bauer, H. J. Gläsel, E. Hartmann, H. Langguth, and R. Hinterwaldner, "Functionalized inorganic/organic nanocomposites as new basic raw materials for adhesives and sealants," *International Journal of Adhesive and Adhesives*, vol. 24, no. 6, pp. 519–522, 2004.
- [5] R. Karthik, K. Gopalakrishnan, R. Venkatesh, A. M. Krishnan, and S. Marimuthu, "Influence of stir casting parameters in mechanical strength analysis of aluminium metal matrix

- composites (AMMCs),” *Material Today Proceeding*, vol. 62, Part 4, pp. 1965–1968, 2022.
- [6] M. Senthil Kumar, L. Natrayan, R. D. Hemanth, K. Annamalai, and E. Karthick, “Experimental investigations on mechanical and microstructural properties of  $\text{Al}_2\text{O}_3/\text{SiC}$  reinforced hybrid metal matrix composite,” *IOP Conference Series: Materials Science and Engineering*, vol. 402, no. 1, 2018.
- [7] R. Venkatesh, C. R. Kannan, S. Manivannan et al., “Synthesis and experimental investigations of tribological and corrosion performance of AZ61 magnesium alloy hybrid composites,” *Journal of Nanomaterials*, vol. 2022, Article ID 6012518, 12 pages, 2022.
- [8] N. Verma and S. C. Vettivel, “Characterization and experimental analysis of boron carbide and rice husk ash reinforced AA7075 aluminium alloy hybrid composite,” *Journal of Alloys and Compounds*, vol. 741, pp. 981–998, 2018.
- [9] R. AM, M. Kaleemulla, S. Doddamani, and B. KN, “Material characterization of SiC and  $\text{Al}_2\text{O}_3$ -reinforced hybrid aluminum metal matrix composites on wear behavior,” *Advanced Composite Letters*, vol. 28, 10 pages, 2019.
- [10] L. Natrayan, M. Singh, and M. Senthil Kumar, “An experimental investigation on mechanical behaviour of SiCp reinforced Al 6061 MMC using squeeze casting process,” *International Journal of Mechanical and Production Engineering Research and Development (IJMPERD)*, vol. 7, no. 6, pp. 663–668, 2017.
- [11] D. Ulutan and T. Ozel, “Machining induced surface integrity in titanium and nickel alloys: a review,” *International Journal of Machine Tools and Manufacture*, vol. 51, no. 3, pp. 250–280, 2011.
- [12] Z. Fattahi, S. A. Sajjadi, A. Babakhani, and F. Saba, “Ni-Cr matrix composites reinforced with nano- and micron-sized surface- modified zirconia: synthesis, microstructure and mechanical properties,” *Journal of Alloys and Compounds*, vol. 817, article 152755, 2020.
- [13] L. Natrayan and M. Senthil Kumar, “Optimization of wear behaviour on AA6061/ $\text{Al}_2\text{O}_3/\text{SiC}$  metal matrix composite using squeeze casting technique–statistical analysis,” *Materials Today: Proceedings*, vol. 27, Part 1, pp. 306–310, 2020.
- [14] F. Li, S. Zhu, J. Cheng, Z. Qiao, and J. Yang, “Tribological properties of Mo and  $\text{CaF}_2$  added SiC matrix composites at elevated temperatures,” *Tribology International*, vol. 111, pp. 46–51, 2017.
- [15] S. M. Sharma and A. Anand, “Friction and wear behaviour of Fe-Cu-C based self-lubricating material with  $\text{CaF}_2$  as solid lubricant,” *Industrial Lubrication and Tribology*, vol. 69, no. 5, pp. 715–722, 2017.
- [16] F. Li, J. Cheng, S. Zhu, J. Hao, J. Yang, and W. Liu, “Microstructure and mechanical properties of Ni-based high temperature solid- lubricating composites,” *Material Science and Engineering A*, vol. 682, pp. 475–481, 2017.
- [17] J. M. Zhen, Y. Han, J. Chen et al., “Influence of Mo and Al elements on the vacuum high temperature tribological behavior of high strength nickel alloy matrix composites,” *Tribology International*, vol. 131, pp. 702–709, 2019.
- [18] L. Natrayan and M. Senthil Kumar, “An integrated artificial neural network and Taguchi approach to optimize the squeeze cast process parameters of AA6061/ $\text{Al}_2\text{O}_3/\text{SiC}/\text{Gr}$  hybrid composites prepared by novel encapsulation feeding technique,” *Materials Today Communications*, vol. 25, article 101586, 2020.
- [19] X. H. Zhang, J. Cheng, M. Niu, H. Tan, W. Liu, and J. Yang, “Microstructure and high temperature tribological behavior of  $\text{Fe}_3\text{Al}-\text{Ba}_{0.25}\text{Sr}_{0.75}\text{SO}_4$  self-lubricating composites,” *Tribology International*, vol. 101, pp. 81–87, 2016.
- [20] B. Li, J. Jia, Y. Gao, M. Han, and W. Wang, “Microstructural and tribological characterization of NiAl matrix self-lubricating composite coatings by atmospheric plasma spraying,” *Tribology International*, vol. 109, pp. 563–570, 2017.
- [21] S. Yogeshwaran, R. Prabhu, L. Natrayan, and R. Murugan, “Mechanical properties of leaf ashes reinforced aluminum alloy metal matrix composites,” *International Journal of Applied Engineering Research*, vol. 10, no. 13, pp. 11048–11052, 2015.
- [22] C. A. I. Bin, Y. F. Tan, H. E. Long, T. A. N. Hua, and X. L. Wang, “Tribological properties of Ni-base alloy composite coating modified by both graphite and TiC particles,” *Transactions of Nonferrous Metals Society of China*, vol. 21, no. 11, pp. 2426–2432, 2011.
- [23] P. W. Leech, X. S. Li, and N. Alam, “Comparison of abrasive wear of a complex high alloy hardfacing deposit and WC- Ni based metal matrix composite,” *Wear*, vol. 294–295, pp. 380–386, 2012.
- [24] C. A. León-Patiño, M. Braulio-Sánchez, E. A. Aguilar-Reyes, E. Bedolla-Becerril, and A. Bedolla-Jacuinde, “Dry sliding wear behavior of infiltrated particulate reinforced Ni/TiC composites,” *Wear*, vol. 426–427, pp. 989–995, 2019.
- [25] M. Srivastava, V. K. Srinivasan, and W. Grips, “Influence of zirconia incorporation on the mechanical and chemical properties of Ni-Co alloys,” *American Journal of Material Science*, vol. 1, no. 2, pp. 113–122, 2011.
- [26] D. B. Miracle, “Metal matrix composites - from science to technological significance,” *Composites Science and Technology*, vol. 65, no. 15–16, pp. 2526–2540, 2005.
- [27] P. S. Bains, S. S. Sidhu, and H. S. Payal, “Fabrication and machining of metal matrix composites: a review,” *Materials and Manufacturing Processes*, vol. 31, no. 5, pp. 553–573, 2015.
- [28] K. Velavan, K. Palanikumar, E. Natarajan, and W. H. Lim, “Implications on the influence of mica on the mechanical properties of cast hybrid ( $\text{Al}+10\%\text{B}_4\text{C}+\text{Mica}$ ) metal matrix composite,” *Journal of Materials Research and Technology*, vol. 10, pp. 99–109, 2021.
- [29] C. H. Xu, G. Y. Wu, G. C. Xiao, and B. Fang, “ $\text{Al}_2\text{O}_3/(\text{W},\text{Ti})\text{C}/\text{CaF}_2$  multi-component graded self-lubricating ceramic cutting tool material,” *International Journal of Refractory Metals and Hard Materials*, vol. 45, pp. 125–129, 2014.
- [30] S. Y. Zhu, F. Li, J. Ma et al., “Tribological properties of  $\text{Ni}_3\text{Al}$  matrix composites with addition of silver and barium salt,” *Tribology International*, vol. 84, pp. 118–123, 2015.
- [31] D. S. Xiong, C. Q. Peng, and Q. Z. Huang, “Development of  $\text{MoS}_2$ - containing Ni-Cr based alloys and their high-temperature tribological properties,” *Transactions of Nonferrous Metals Society of China*, vol. 8, no. 2, p. 2269, 1998.